processes

MDPI

Article

# Molecular Recognition and Cell Surface Biochemical Response of *Bacillus thuringiensis* on Triphenyltin

**Hongling Zhang, Jinshao Ye, Huaming Qin, Xujun Liang and Yan Long ***

Guangdong Key Laboratory of Environmental Pollution and Health, School of Environment, Jinan University, Guangzhou 510632, China; honglingzhang12345@163.com (H.Z.); folaye@126.com (J.Y.); huamingqin@163.com (H.Q.); xujun.liang@jnu.edu.cn (X.L.)

* Correspondence: tlongyan@jnu.edu.cn; Tel.: +86-1591-315-2627

Received: 29 April 2019; Accepted: 5 June 2019; Published: 10 June 2019


**Abstract:** Triphenyltin (TPT) has severely polluted the environment, and it often coexists with metal ions, such as $Cu^{2+}$. This paper describes the cell's molecular recognition of TPT, the interaction between TPT recognition and $Cu^{2+}$ biosorption, and their effect on cell permeability. We studied the recognition of TPT by *Bacillus thuringiensis* cells and the effect of TPT recognition on $Cu^{2+}$ biosorption by using atomic force microscopy to observe changes in cell surface mechanical properties and cellular morphology and by using flow cytometry to determine the cell growth status and cell permeability. The results show that *B. thuringiensis* can quickly recognize different media. The adhesion force of cells in contact with Tween 80 was significantly reduced to levels that were much lower than that of cells in contact with PBS. Conversely, the cell surface adhesion force increased as TPT became more degraded. *B. thuringiensis* cells maintained their original morphology after 48 h of TPT treatment. The amount of $Cu^{2+}$ adsorption by TPT-treated cells was positively correlated with the surface adhesion force ($r = 0.966$, $P = 0.01$). The cell adhesion force significantly decreased after $Cu^{2+}$ adsorption, and cell recognition of TPT and/or $Cu^{2+}$ hindered the entrance of 2′,7′-dichlorodihydrofluorescein diacetate (DCFH-DA) into the cell. The initial diffusion time of DCFH-DA into cells treated by PBS, $Cu^{2+}$, TPT, and TPT+$Cu^{2+}$ was 4, 10, 30, and 30 min, respectively, and the order of the fluorescence intensity was PBS >> $Cu^{2+}$ > TPT > TPT+$Cu^{2+}$. We conclude that changes in the cell surface properties of the microbe during recognition of pollutants depend on the contaminant's properties. *B. thuringiensis* recognized TPT and secreted intracellular substances that not only enhanced the adsorption of $Cu^{2+}$, but also formed a "barrier" on the cell surface that reduced permeability. These findings provide a novel insight into the mechanism of microbial removal of pollutants.

**Keywords:** Triphenyltin; molecular recognition; mechanical properties; biodegradation; biosorption

## 1. Introduction

With the continuous improvement of people's living standards and the development of cities, environmental pollution is becoming increasingly worse. Organotin is an organometallic compound that is widely used in agriculture, industry, textiles, transportation, and other related fields [1–3]. Triphenyltin (TPT), a representative organotin that elicits endocrine behavior in cells [4], has contaminated environments worldwide [5], severely affecting ecological systems and sustainable development.

The microbial treatment of TPT has been widely investigated. Multiple strains with high degradation performance, including *Stenotrophomonas maltophilia* [6], *Brevibacillus brevis* [7], and *Bacillus thuringiensis*, have been screened for their ability to degrade organotins. Several studies have revealed that the mechanisms of TPT biodegradation result in diphenyltin (DPT), monophenyltin (MPT), and tin as degradation products [8]. Endoenzymes, an appropriate amount of exogenous

nutrients, and surfactants can accelerate TPT degradation [8–10]. Furthermore, the protein expression of *B. thuringiensis* and its metabolic network related to the degradation of pollutants, such as erythromycin and triclosan, have been revealed by using omics approaches [11,12]. However, the mechanisms by which *B. Thuringiensis* recognizes and adsorbs copper after TPT treatment have not been reported.

Metallic ions, such as copper, often coexist with TPT and tributyltin (TBT) in the environment. However, the combined effect of Cu and TPT has not been rigorously studied, and conclusions of their interaction and toxicity to organisms have not been consistent among studies using different prediction models. For marine organisms, the interaction between TPT and Cu was determined to be antagonistic according to the Loewe parametric response surface model (CARS), while it was found to be synergistic on the basis of the response additive response surface model (RARS) [13]. Hence, the effect of the interaction between TPT and Cu on organisms is still unclear. Moreover, the adsorption and recognition of metal ions by *B. thuringiensis* have not been reported.

In addition to imaging, the interaction between cells and contaminants can be revealed by the cell's mechanical properties, including information on deformation, Young's modulus, adhesion force, and energy dispersion [14]. Young's modulus, also referred to as the elastic modulus, tensile modulus, or modulus of elasticity in tension, is the stress-to-strain ratio and equal to the slope of a stress–strain diagram for the material of interest [14]. The adhesion force and roughness can reflect the change in cells exposed to external stress. Atomic force microscopy (AFM) has advantages in quantifying the mechanical properties of biological specimens [15,16] and is suitable for observing and characterizing the nanoscale morphology of a sample surface. In the field of biology, AFM is mainly used to observe the surface ultrastructure of biological macromolecules, cells, microbes, and viruses and quantitatively determine surface mechanical properties. For example, a nanoscale imaging method that employs AFM was invented to dynamically observe microbial growth in situ during the process of splitting in real time [17]. The root-mean-square roughness of Bucky paper was found to increase as a result of *B. thuringiensis* cells' adherence to the surface to form biofilm [18]. AFM can also be used to investigate cell recognition. The surface force interaction between cells and a metal surface was previously determined by AFM, and the results revealed the process of biofilm formation by three bacterial species on stainless steel 316 [19]. The lateral separation force of *Escherichia coli* [20] and the binding force between bacterial and cytoplasmic membranes [21] were also detected using AFM. Therefore, it has been widely accepted that AFM can be used to detect the changes in mechanical properties and micro morphology that result from the interaction between the probe and the cells, and these observations can confirm changes in the sample surface structure.

Molecular recognition is the initial step in TPT or metal ion adsorption, degradation, and accumulation. Observing a microbe's recognition process of pollutants is vital to understanding the interaction between binary pollutants and the resulting toxicity to organisms. How does a cell recognize target pollutants? What is the cell's response to pollutants to mitigate harm? In this study, Young's modulus, adhesion force, roughness, average particle height, and cell morphology were measured in cells to characterize the process by which *B. thuringiensis* recognizes different media, including organotin molecules with different structures. The cell recognition mechanism of *B. thuringiensis* exposed to the combined pollution of TPT and Cu was also studied; the results provide a novel insight into the performance of microbes in the presence of binary pollutants.

## 2. Materials and Methods

### 2.1. Strain and Chemicals

*Bacillus thuringiensis* was isolated from organotin-contaminated sediment samples collected from an e-waste processing and recycling town called Guiyu in Guangdong Province, China [8]. TPT, DPT, MPT, and Chromatographic methanol were purchased from Sigma-Aldrich (St. Louis, MO, USA).

Lysogeny broth used for cell cultures contained beef extract, NaCl, and peptoneat concentrations of 3, 5, and 10 g·L$^{-1}$, respectively. The concentrations of $KH_2PO_4$, NaCl, $NH_4Cl$, and $MgSO_4$ in the mineral salt medium (MSM) were 30, 20, 30, and 10 mg·L$^{-1}$, respectively.

Beef extract, NaCl, peptone, $KH_2PO_4$, $NH_4Cl$, $MgSO_4$, Tween 80, phosphate-buffered saline (PBS), and $CuCl_2$ were of analytical grade and purchased from Guangzhou Chemical Reagent Factory. Consumables, such as 0.22 μm filter membranes, mica plates, and 1 mL disposable syringes, were purchased from Guangzhou Dongzheng Chemical Glass Instrument Co., Ltd. (Guangzhou, China).

### 2.2. Microbial Culture

*B. thuringiensis* was inoculated into 250 mL Erlenmeyer flasks containing 100 mL of culture medium and incubated at 30 °C on a rotary shaker at 120 r·min$^{-1}$ for 12 h. Subsequently, the cells were separated from the culture medium by centrifugation at 3500× *g* for 10 min for further experiments. The cellular growth phases were determined by the OD at 600 nm. The relation between the cellular growth phases and TPT treatment was investigated by varying the culture time from 0 to 48 h.

### 2.3. Mechanical Properties Analysis of Bacillus thuringiensis upon Recognizing Different Media

The separated cells were added to 20 mL of the MSM at the final cell concentration of 1 g·L$^{-1}$. After shaking, 0.1 mL of the sample was pipetted through a disposable syringe over a 0.22 μm polyether sulfone filter followed by successively washing with sterile phosphate-buffered saline (PBS), $2.597 \times 10^{-3}$ mol·L$^{-1}$ TPT solution, and 50 mg·L$^{-1}$ of Tween 80 solution three times to characterize the cells' quick recognition process of these media. The filter membrane was removed, and the bacteria were allowed to attach to gel-modified mica and naturally air-dry [22]. Using PBS as the liquid medium, the Young's modulus and the surface adhesion force of the samples were quantitatively determined by atomic force microscope (AFM). In addition, part of the suspension after shaking was ultrasonically disrupted in an ice bath using an ultrasonic cell pulverizer (the working time was 6 s, the interval time was 9 s, the total time was 30 min, and the ultrasonic power was 450 W), and the sample was crushed at 25 °C, centrifuged at 12,000× *g* for 5 min, and the supernatant was taken as the cytoplasm (intracellular fluid). In addition, the cells were collected and dried according to the steps followed for characterizing the rapid recognition process. After the cells on the gel-modified mica chip were naturally dried, PBS (control), cytoplasm, 1% methanol solution, $2.597 \times 10^{-3}$ mol·L$^{-1}$ TPT solution, or $2.597 \times 10^{-3}$ mol·L$^{-1}$ TPT/1% methanol solution were added as the liquid medium, and Young's modulus and surface adhesion force were measured by AFM to characterize the cell's conventional recognition of different substances (about 12 min).

Using the same molar concentrations of TPT, DPT, and MPT, Young's modulus and surface adhesion force were measured by AFM using PBS as a liquid medium. The specific steps were the same as those followed to characterize the conventional recognition process.

### 2.4. Cellular Morphology

The cells were collected in a 1.5 mL centrifuge tube and appropriately diluted with PBS. The 10 μL diluted samples and control samples were added to the newly stripped mica chip and rapidly, naturally air-dried. The control sample consisted of cells that were not washed.

Subsequently, the samples were mounted onto the XY stage, and an integral video camera was used to locate the observed regions. The imaging experiments were conducted in the tapping mode using a microfabricated silicon cantilever (Park Scientific Instruments, Autoprobe CP, American thermoelectric Co., Ltd. USA). The image data were smoothed using the software NanoScope Analysis Version 1.20 to eliminate low-frequency background noise in the scanning direction. A1 × 1 μm area in the middle of each group of test cells was further selected for detailed scanning to determine the surface roughness and average particle height of *B. thuringiensis.*

### 2.5. Effect of TPT on Cell Recognition of $Cu^{2+}$

The cells were added to 20 mL of the MSM for a final cellular concentration of 1 g·$L^{-1}$. Subsequently, TPT stock solution dissolved in chromatographic grade methanol was pipetted into the medium, in which the final concentration of TPT was 2.597 × $10^{-3}$ mol·$L^{-1}$. All samples were cultured in the dark at 30 °C on a rotary shaker at 120 r·$min^{-1}$. Cells from the two groups of samples were collected at 0, 0.5, 2, 12, 24, and 48 h to observe cellular morphology and mechanical properties by AFM. To determine whether the TPT-induced change in atomic force of the cellular surface altered molecular recognition, cells at different time points after TPT degradation were assessed for their adsorption of $Cu^{2+}$. The biosorption experiment, which used 10 µmol·$L^{-1}$ $Cu^{2+}$ and 1 g·$L^{-1}$ *B. thuringiensis*, was performed in the dark at 30 °C in 20 mL of the treatment solution with shaking on a rotary shaker at 120 r·$min^{-1}$ for 60 min. After treatment, the cells were separated by centrifugation at 3500× *g* for 5 min and the mechanical properties were detected. Residual $Cu^{2+}$ in the resultant supernatant was detected by an atomic flame absorption spectrophotometer (SHIMADZU AA-7000) to determine the amount of biosorption. Blank controls were run in parallel in flasks that were not inoculated, and experimental controls were established by using cells without the addition of $Cu^{2+}$.

Meanwhile, *B. thuringiensis* cells were harvested from the TPT and MSM system after 12 h to reveal the effect of the adsorption time on the amount of $Cu^{2+}$ adsorbed by the cells. The experimental adsorption times for 10 µmol·$L^{-1}$ $Cu^{2+}$ and 1 g·$L^{-1}$ cells were 15, 30, 45, 60, 75, 90, 105, and 120 min.

### 2.6. Effect of TPT and Copper on Cells

Cells that had degraded TPT for 12 h were assessed for their ability to adsorb $Cu^{2+}$ for 60 min. Subsequently, these cells and the control cells, after centrifugation at 3500× *g* for 5 min, were suspended in 2′,7′-dichlorodihydrofluorescein diacetate (DCFH-DA) to obtain a cell concentration of approximately $10^6$ cells per mL. Samples were then detected every few minutes by a Flow Cytometer (FCM, Beckman Coulter, Brea, CA, USA) and analyzed with Kaluza for Gallios Software. Each sample was analyzed by alaser beam at an excitation wavelength of 488 nm. The detector-measured emission intensity was set at 525 nm.

### 2.7. Statistical Analysis

All of the experiments were performed in triplicate, and the mean values were used in the calculations. The statistical analysis of the correlation between the adhesion force of *B. thuringiensis* and phenyltin degradation was performed by SPSS version 13.0 using Pearson correlation tests.

## 3. Results and Discussion

### 3.1. Recognition and Binding of Different Compounds

Figure 1 shows that the cells quickly recognized different media. The roughness of the cell surface after contact with PBS, TPT solution, and Tween 80 solution in the rapid contact process was 6.35 ± 1.07, 6.29 ± 0.93, and 2.53 ± 0.48 nm, respectively, and the average particle height was 12.76 ± 0.46, 11.97 ± 0.76, and 8.50 ± 0.98 nm. After the quick contact process with Tween 80, the adhesion force of the cells was significantly lower than that of the cells exposed to the control (PBS), and the Young's modulus of the former was increased (Figure 1b). However, there was no significant difference in adhesion force and Young's modulus between cells exposed to the PBS and TPT solution (Figure 1b). These results indicate that changes in cell surface properties after recognition of pollutants are related to the contaminant's properties. Owing to the solubilization of Tween 80, hydrophobic organic compounds are dissolved, and more molecule metabolites on the cell surface are transferred to the solution, thereby reducing the surface adhesion force of the cells. Consequently, the cell surface roughness and average particle height decreases, and the surface of the cells in contact with Tween 80 becomes relatively smooth (Figure S1d). However, 1 L of water dissolve only 0.14 mg TPT at 25 °C [9],

and the cell cannot recognize TPT in a very short time; thus, there was no significant difference between the PBS and TPT solutions.

The frequency of Young's modulus, which represents the trend of the change in the scanning interaction force as the distance varies between the probe tip and the sample, follows a normal distribution (Figure 1b). Therefore, the force data distribution is concentrated and the results are reliable. Figures S2 and S3 also confirm this conclusion. In the conventional contact experiment, the Young's modulus and adhesion force of the cells in contact with the 1% methanol solution were similar to those of the control cells, with values of 915 ± 50 and 902 ± 49 kPa (Young's modulus) and 369 ± 17 and 334 ± 22 pN (adhesion force), respectively (Figure 1c). The cell surface adhesion forces of the strains in contact with TPT solution, TPT/methanol solution, and cytoplasm were 373 ± 19, 459 ± 21, and 719 ± 20 pN (Figure 1c), respectively, which are significantly higher than that of the control. The Young's modulus of the cells in contact with the TPT/methanol solution and cytoplasm was significantly decreased, which indicates that *Bacillus thuringiensis* recognized TPT within a short time. The methanol solution had no obvious effect on the cell surface properties, but it did promote the recognition of TPT by the cells, which may be the result of the improved TPT solubility by methanol. TPT can induce cells to secrete intracellular substances [23] (mainly proteins) to resist the negative effect of TPT on cells. Therefore, TPT may be recognized by *B. thuringiensis* through extracellular secretions. The change in cell surface adhesion force in the cytoplasm during the conventional recognition process also supports this inference.

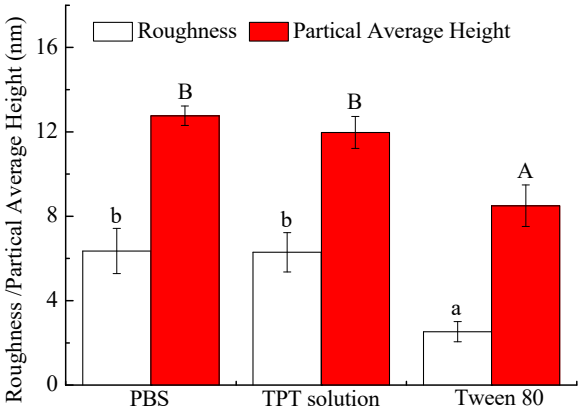


(**a**)

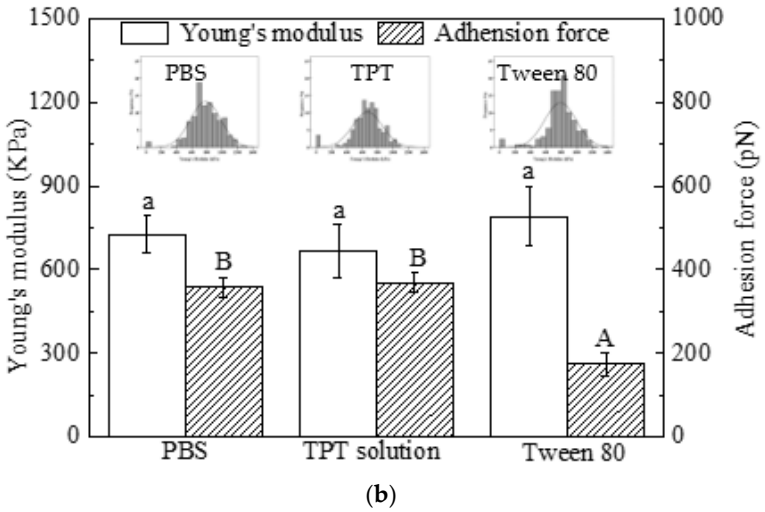


(**b**)

**Figure 1.** *Cont.*

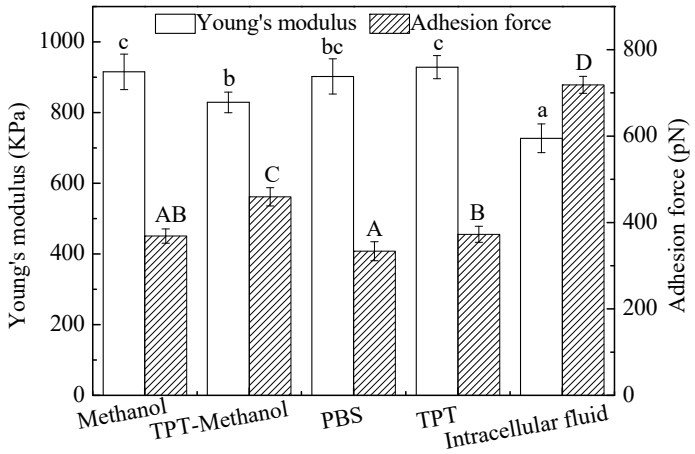


(**c**)

**Figure 1.** Pollutant recognition and contact process. (**a**) Roughness and average particle height of *Bacillus thuringiensis* during the quick contact process; (**b**) Young's modulus and adhesion force of *B. thuringiensis* during the quick contact process. The normal distribution curve of the Young's modulus frequency indicates that the distribution of force data is concentrated and the results are reliable. (**c**) Young's modulus and adhesion force of *B. thuringiensis* during the conventional contact process. The same lowercase letter indicates that there was no significant difference among the groups ($P > 0.05$), and different lowercase letters represent a significant difference among the groups ($P < 0.05$). The same meaning applies to capital letters. Lowercase letters represent significant differences in roughness in (**a**), and capital letters represent significant differences in average particle height. Lowercase and capital letters represent significant differences in Young's modulus and adhesion force in (**b**) and (**c**), respectively.

### 3.2. Effect of TPT on Cellular Morphology of Bacillus thuringiensis

As demonstrated in Figure 2, there was no significant difference in cellular morphology in the presence or absence of TPT within 2 h. Yet, an obvious difference in cell morphology was observed between the control and experimental groups from 12 to 48 h. Without TPT in the MSM system, the cell gradually collapsed and shrank (Figure 2c1,d1,e1) because of the lack of a carbon source in the MSM system. As the culture time was prolonged, the cells grew and reproduced, and the carbon source in the system was decreased and ultimately exhausted; then, the cells gradually ruptured, and the cytoplasm was released. However, in the TPT system, the cells maintained their original morphology (Figure 2c2,d2,e2). This is because *B. thuringiensis* can degrade TPT [8] and use it as a carbon source to maintain growth. Although the surface of the cells shrank and the intracellular matter decreased with the degradation time, the damage was much less compared with the damage to cells without TPT in the system. TPT inhibited the growth of *B. thuringiensis* to a certain extent (Table S1): the growth and metabolism of cells slowed down during the process of TPT degradation, and the rate of carbon source utilization in the system decreased.

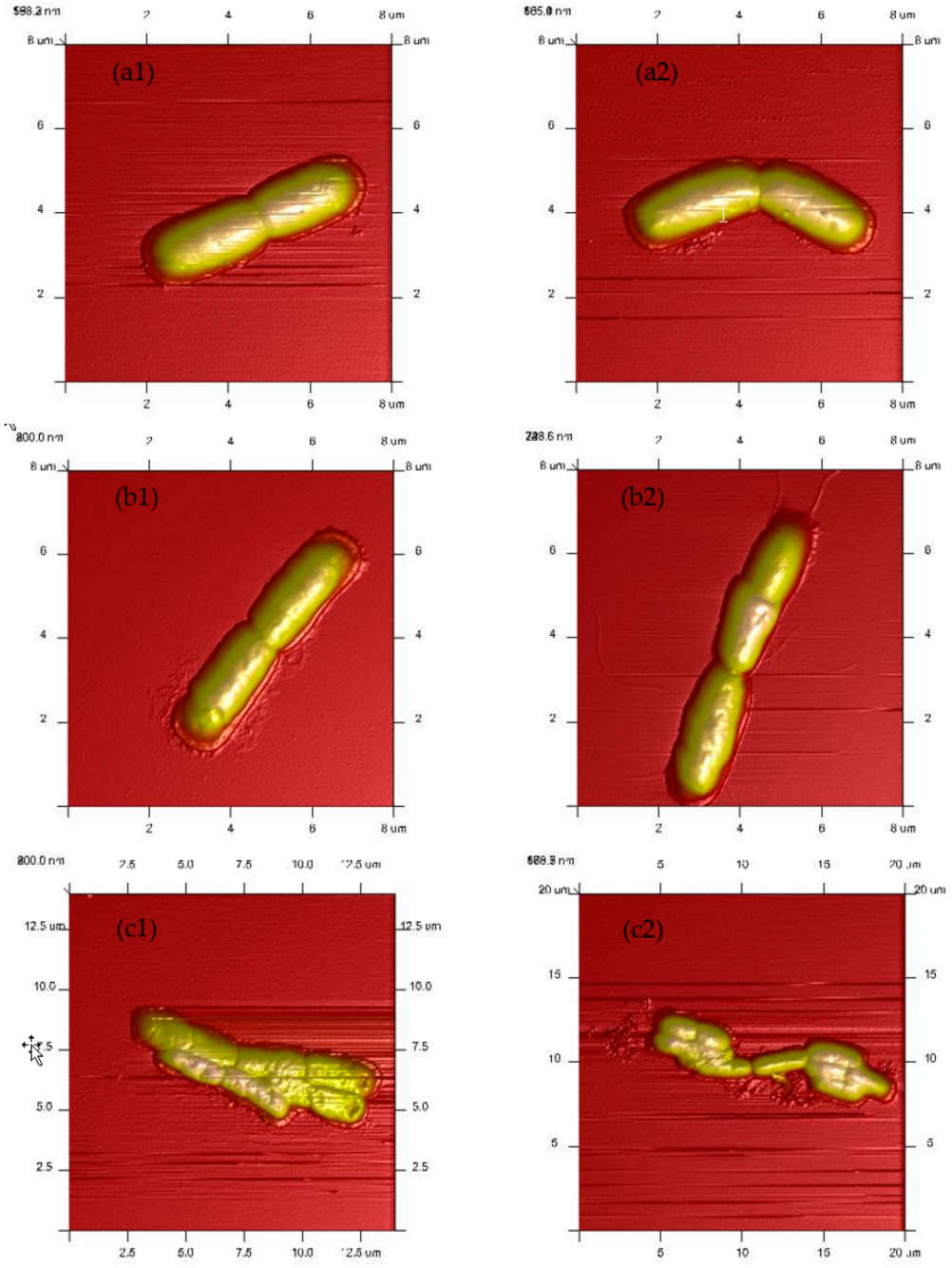


**Figure 2.** *Cont.*

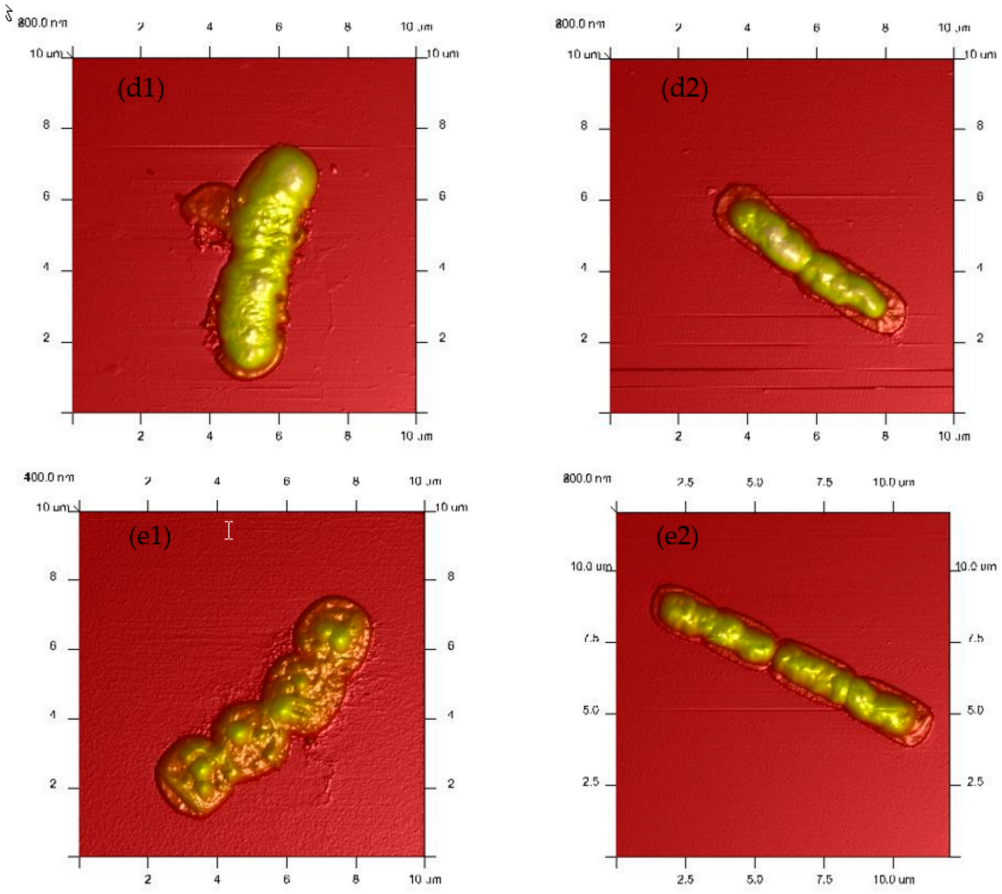


**Figure 2.** Morphology of *B. thuringiensis* during TPT biodegradation. (**a1**), (**b1**), (**c1**), (**d1**), and (**e1**) indicate the sample in the MSM system at 0, 2, 12, 24, and 48 h, respectively, and (**a2**), (**b2**), (**c2**), (**d2**), and (**e2**) represent the sample in the solution with TPT at 0, 2, 12, 24, and 48 h, respectively.

### *3.3. Changes in Mechanical Properties of Bacillus thuringiensis during Biodegradation of Phenyltin*

The Young's modulus of the *B. thuringiensis* cell surface decreased from 707 ± 29 kPa at 0 h to 570 ± 20 kPa after degrading TPT for 48 h (Figure 3a). The cell surface adhesion force increased significantly to 704 ± 25 pN within 12 h. Afterward, the growth rate slowed, and the adhesion force reached 750 ± 23 pN at 48 h. Combined with cellular morphology changes (Figure 2), we can infer that the increase in adhesion force was mainly caused by active secretions, rather than the outflow of intracellular substances. It has been reported that TPT can be rapidly adsorbed by the cell surface through physicochemical interactions, such as electrostatic attraction, cell affinity, and ion exchange [24]. Then, TPT can easily penetrate the cell wall [9] and be transferred to the cytoplasm through active transport [25], stimulate the cell to secrete intracellular substances [23] (mainly proteins) to cover the cell surface, increase the cell surface adhesion force, and reduce the Young's modulus of the cell surface. According to the growth of the cells (Table S1) during TPT degradation, the cell biomass increased markedly in the first 12 h but slowly after 12 h, at which point it tended to be stable. Meanwhile, TPT biosorption by the cell surface showed an increasing trend with in the first 12 h and then decreased from 12 to 24 h, gradually stabilizing thereafter. TPT degradation efficiency increased gradually (Table S1), which illustrates that the biosorption of TPT by cells is related to the initial concentration of TPT and the biomass of the cells and that degradation efficiency is probably dependent on the cell biomass and ability of the individual cells. As the cell proliferation slowed and the remaining TPT concentration in the system decreased, the amount of TPT adsorption decreased, while the degradation efficiency was gradually enhanced, which reveals that more TPT was degraded per individual cell. Furthermore, the cell surface adhesion force was linearly positively correlated with the TPT, DPT,

and MPT degradation rate (r = 0.948, $p$ = 0.05; r = 0.972, $p$ = 0.01; r = 0.967, $p$ = 0.01; Table S2), which indicates that the higher the cell surface adhesion force, the stronger the degradation ability of individual cells. TPT is degraded intracellularly [23], which indirectly supports the hypothesis that intracellular secretions recognize TPT. This is further verified by the change in the adhesion force of *B. thuringiensis* during the degradation of TPT, DPT, and MPT (Figure 3b). The cell adhesion force in the presence of TPT, DPT, and MPT increased rapidly from 387 ± 30, 356 ± 25, and 350 ± 25 pN to 704 ± 25, 518 ± 25, and 503 ± 24 pN during the first 12 h, respectively. After 12 h, the adhesion force tended to be stable. The adhesion force of cells treated with TPT was significantly higher than that of DPT- and MPT-treated cells, which may be a consequence of the differences in biodegradability of the three compounds. The more complex the structure of the compound, the more slowly it is degraded [8]. Since TPT has the most complex structure, it is more difficult for *B. thuringiensis* to utilize. Its benzene-containing metabolites inhibit the oxidation of TPT, which causes the cell to secrete more viscous substances to promote TPT degradation.

Although the mechanical properties vary among the phenyltins used in this study (Figure 3b), there was no correlation between adhesion force, molecular weight, molecular size, and twist angle (Table S3), which demonstrates that the changes in the cells' mechanical properties are dependent on the interaction between the pollutants and the cells. It has been verified that the recognition and binding of TPT by functional proteins depend on a protein's specific amino acid sequences but not its advanced structure [26]. Organisms that contain the same genes or proteins exhibit the same or similar responses to TPT, and the effective biosorption, transport, and degradation of TPT by *Brevibacillus brevis* support the above deduction [7].

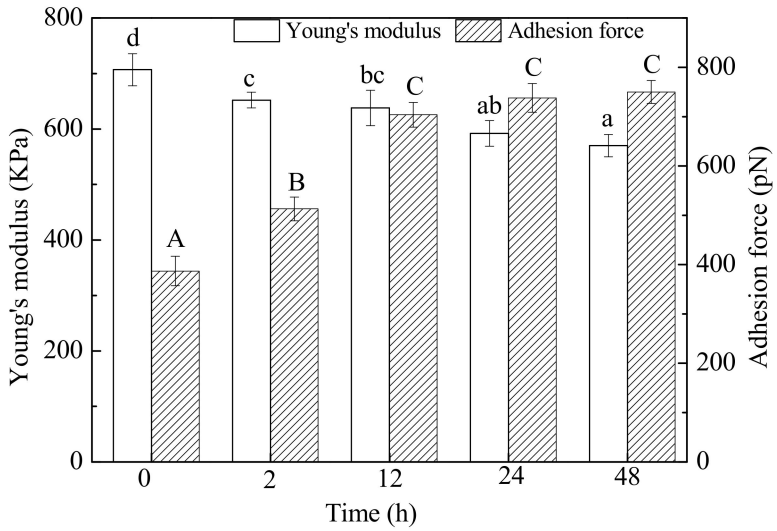


(**a**)

**Figure 3.** *Cont*.

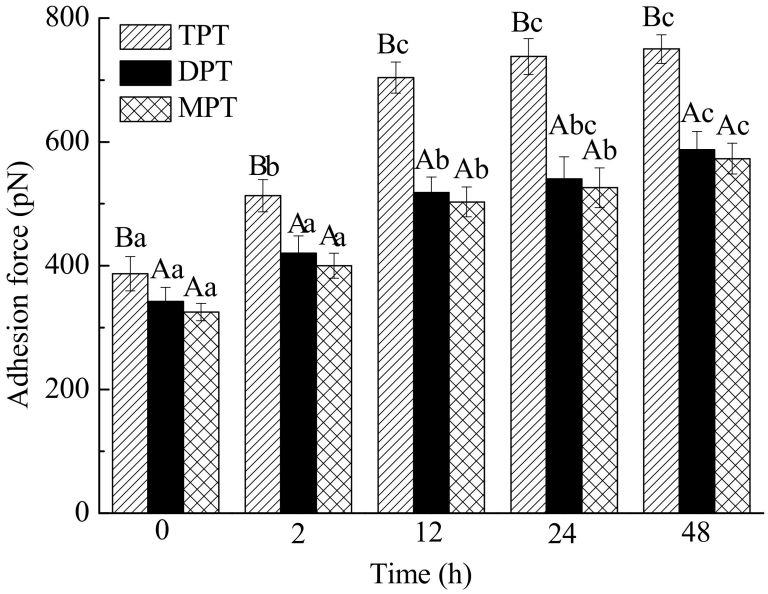


(**b**)

**Figure 3.** Change inmechanical properties of *B. thuringiensis*. (**a**) Change in mechanical properties in the TPT biodegradation process; (**b**) Adhesion force of *B. thuringiensis* during phenyltin biodegradation. The same lowercase letter indicates that there was no significant difference among the groups ($P > 0.05$), and different lowercase letters represent a significant difference among the groups ($P < 0.05$). The same meaning applies to capital letters. Lowercase and capital letters represent a significant difference in Young's modulus and adhesion force in (**a**), respectively. Lowercase letters represent a significant difference for the substance at different times; capital letters represent a significant difference for substances at the same time in (**b**).

### *3.4. Effect of TPT on $Cu^{2+}$ Recognition by Bacillus thuringiensis*

The ability of TPT-treated cells to adsorb $Cu^{2+}$ was greatly enhanced (Figure 4a), and the removal efficiency reached 80% after 2 h, which is significantly higher than that of the control group (60%). *B. thuringiensis* cells have surface chemical functional groups, such as amino, carboxyl, hydroxyl, and carbonyl groups, which can carry negative charges [27]. Thus, $Cu^{2+}$, with a high affinity and positive charge, is rapidly attracted to the cell surface [28]. It can be inferred that the increase in $Cu^{2+}$ adsorption is associated with the increase in viscous substances on the cell surface. $Cu^{2+}$ biosorption by cells treated with TPT for different times also supports this interpretation (Figure 4b). $Cu^{2+}$ biosorption rose with the TPT treatment time within 12 h and became relatively stable after 12 h. Moreover, $Cu^{2+}$ biosorption (Figure 4b) consistently improved with the increase in adhesion force (Figure 4c). It has been demonstrated [29] that viscous substances on the cell surface can increase the hydrophobicity of cells, while the hydrophobic behavior of cells enhances the adsorption of $Cu^{2+}$ because of its positive charge. The adhesion force of cells treated with TPT and $Cu^{2+}$ was significantly lower compared with cells not exposed to $Cu^{2+}$ (Figure 4c). The removal efficiency of $Cu^{2+}$ (Figure 4a) was positively correlated with the surface adhesion force (Figure 3a) ($r = 0.966$, $P = 0.01$; Table S2), which suggests that the enhancement of $Cu^{2+}$ biosorption was due to the increase in cell surface viscosity. The cell surface roughness and average particle height of cells after $Cu^{2+}$ adsorption were also increased (Figure 4d), further supporting the above inference.

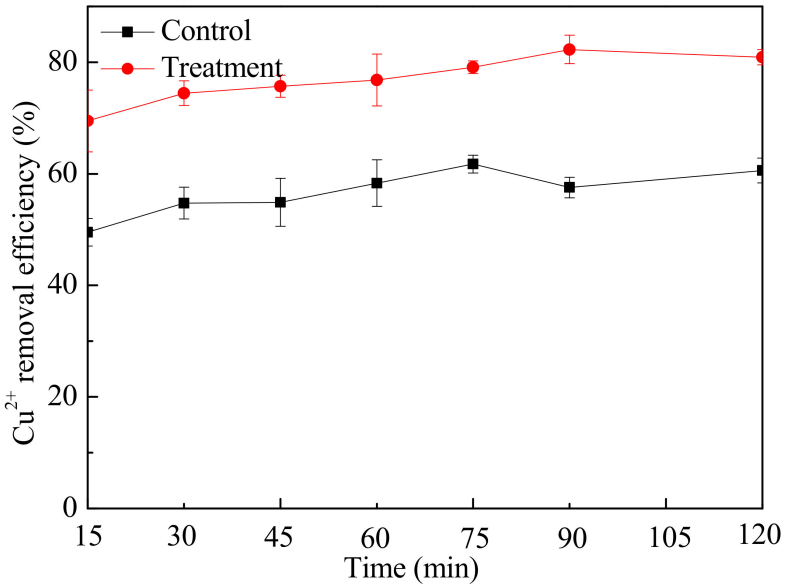


(**a**)

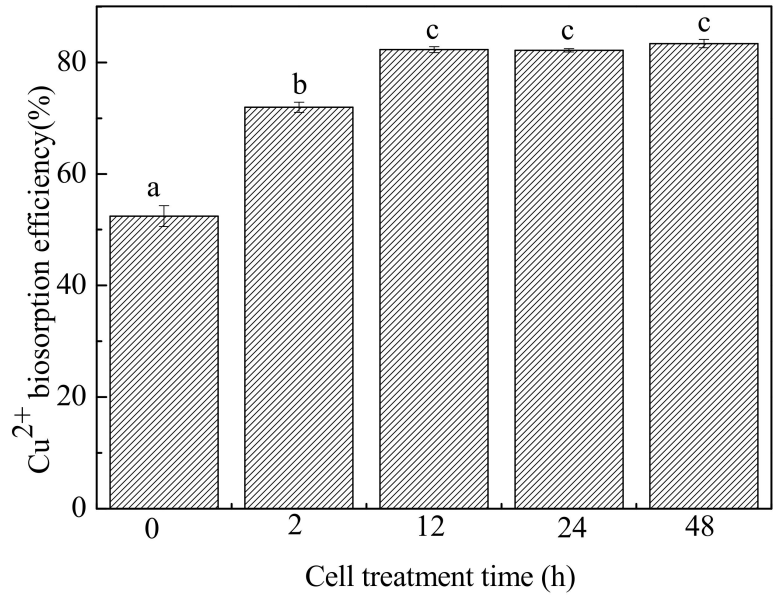


(**b**)

**Figure 4.** *Cont.*

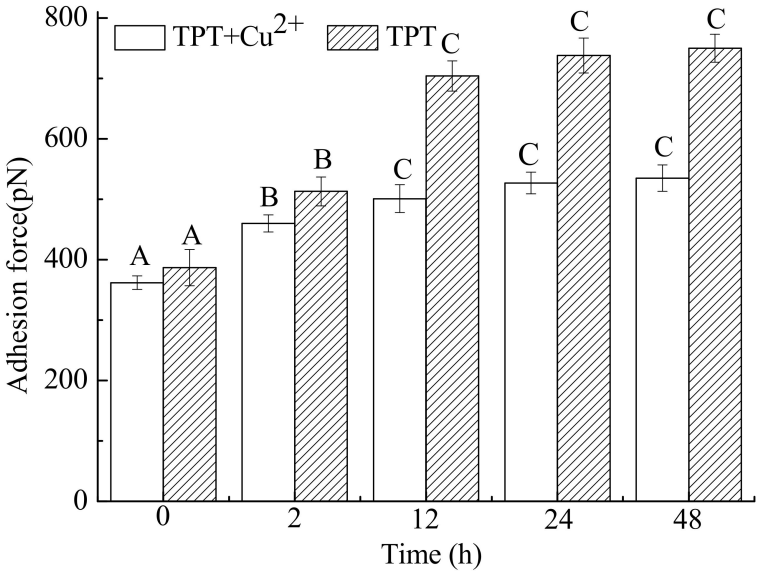


(**c**)

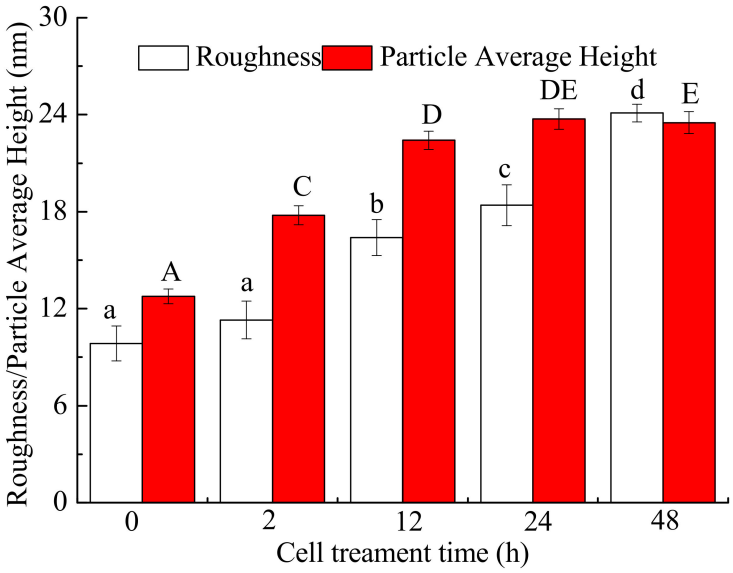


(**d**)

**Figure 4.** $Cu^{2+}$ biosorption. (**a**) Effect of absorption time on $Cu^{2+}$ removal efficiency. "Control" indicates cells in MSM for 12 h and "Treatment" indicates cells that degraded TPT for 12 h. (**b**) $Cu^{2+}$ biosorption efficiency of *B. thuringiensis* under different treatment times of TPT. (**c**) The change in adhesion force with or without $Cu^{2+}$ during TPT biodegradation. Lowercase letters represent significance for the same substance at different times; capital letters represent significance for different substances at the same point in time. (**d**) Surface roughness and average particle height of *B. thuringiensis* after $Cu^{2+}$ biosorption for 60 min with different TPT treatment times. The same lowercase letter indicates that there was no significant difference among the groups ($P > 0.05$), and different lowercase letters represent a significant difference among the groups ($P < 0.05$). The same meaning applies to capital letters. Lowercase and capital letters represent a significant difference in roughness in (**a**) and average particle height, respectively.

### *3.5. Cell Surface Response to the Combination of Triphenyltin and Copper Ions*

DCFH-DA has no fluorescence and can cross the cell membrane freely. When DCFH-DA enters the cell, it is hydrolyzed by intracellular esterase into DCFH. DCFH does not penetrate the cell membrane, so the probe easily accumulates in the cell to produce fluorescence.

The intracellular fluorescence intensity of *B. thuringiensis* exposed to different treatments is shown in Figure 5. The order of fluorescence intensity for the different treatments was control >> $Cu^{2+}$ > TPT > TPT+$Cu^{2+}$. The fluorescence intensity of the control group increased sharply before 60 min, after which it tended to be stable. In the other groups, the intracellular fluorescence intensity increased slowly over a period of 120 min. Moreover, the time at which the onset of obvious changes in fluorescence intensity occurred differed among the different groups: the onset of the fluorescence intensity change of the control, the cells adsorbing $Cu^{2+}$, the cells treated with TPT, and the cells treated with TPT+$Cu^{2+}$ was 4, 10, 30, and 30 min, respectively. This suggests that *B. thuringiensis* cells had reduced membrane permeability after their contact with the pollutants. Obviously, the effect of TPT on cell membrane permeability was stronger than that of $Cu^{2+}$. This may be related to the change in the cell surface characteristics of *B. thuringiensis*.

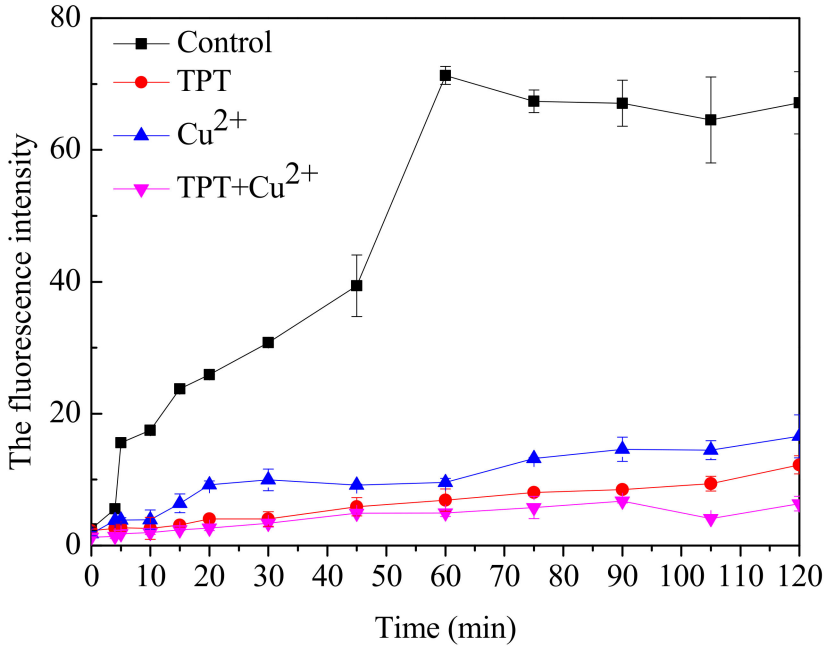


**Figure 5.** The fluorescence intensity of *B. thuringiensis*. Reactions occurred at 30 °C in darkness at different times.

Generally, most DCFH-DA molecules can pass through the cell membrane freely by free diffusion in 20 min. In this study, the intracellular fluorescence of the control group increased sharply with the prolongation of time to 60 min, which indicates that DCFH-DA entered the cell gradually. The cell number, cell surface structure, and cell membrane permeability had an effect on the change in fluorescence intensity. From the fluorescence intensity change for the $Cu^{2+}$ adsorption treatment group, we can conclude that the cell number had little effect on the change in fluorescence intensity. Previous research has reported that TPT can increase the cell membrane permeability of *B. thuringiensis* [30]. In this study, according to the change in fluorescence intensity in the $Cu^{2+}$, TPT, and TPT+$Cu^{2+}$ groups, it can be deduced that the changes in cell surface structure were the main reason for fluorescence intensity changes. The adsorbed layer on the cell surface might form a barrier and block other material from entering the cell interior. Obviously, the barrier caused by TPT was stronger than that caused by $Cu^{2+}$, indicating that the intercellular secretion induced by TPT was the more effective

shell. The change in the surface morphology of cells treated by TPT+$Cu^{2+}$ also supports this inference (Figure S4). Bacteria in a biofilm state are more resistant to harmful conditions and substances, such as adverse growth environments and antibiotics, compared with bacteria in a free state [31]. After contact with TPT, the cells secreted viscous substances on the cell surface to form a biofilm, which prevented DCFH-DA from entering the cells. This was especially the case for the cells that adsorbed $Cu^{2+}$; in these cells, a shielding layer was formed, which further hindered DCFH-DA from nearing the cell surface. In this treatment, the toxicity of the combined pollution of $Cu^{2+}$ and TPT was less than that which would result from an additive response of individual $Cu^{2+}$ and TPT treatments.

During its degradation, TPT induces *B. thuringiensis* to secrete viscous substances, and the main component of these secretions may be copper-related proteins. In the early stage of our research, *B. thuringiensis* was completely sequenced, and various protein types in the cells were obtained from the results of sequencing. The functional proteins related to copper ions that were obtained by screening are shown in Table S4. During the degradation of TPT, the protein secreted by *B. thuringiensis* in response to TPT and the protein flow out of the cells caused an increase in cell surface adhesion force, and the increase in adhesion force was significantly correlated with the biosorption of $Cu^{2+}$ by TPT (Table S2). This indicates that the proteins on the surface of the cells can be complexed with $Cu^{2+}$, and this improved $Cu^{2+}$ biosorption efficiency (Figure 4a,b). Therefore, the viscous substances on the surfaces of the cells are likely to be three types of proteins: Cytochrome oxidase biogenesis protein (Sco1), Cytoplasmic copper homeostasis protein (CutC), and Copper chaperone (CopZ).

## 4. Conclusions

*Bacillus thuringiensis* recognized different media, and the change in cell surface properties was related to the medium's characteristics. After the cells recognized Tween 80, the adhesion force of the cell surface decreased and Young's modulus increased. As the cells recognized TPT, they secreted intracellular substances and released them to the cell surfaces, which increased the cell surface adhesion force and decreased the Young's modulus. Moreover, the increase in the adhesion force of cells was related to the biodegradability of the organotin; the adhesion force of those treated by TPT was significantly greater than that of those treated by DPT and MPT. Though the amount of TPT adsorbed by cells decreased with time, the degradation efficiency increased. There was a positive correlation between degradation efficiency and cell surface adhesion force. Secretions stimulated by TPT promoted the adsorption of $Cu^{2+}$ by cells, and the adsorption efficiency of $Cu^{2+}$ by cells was increased by nearly 20%. Both $Cu^{2+}$ and TPT hindered other materials from passing the cell membrane; however, the shielding effect of TPT was much stronger than that of $Cu^{2+}$. The cell secretions of *Bacillus thuringiensis* induced by TPT not only facilitated the degradation of TPT but also formed a barrier to hinder the entry of DCFH-DA into the cells. This shielding effect was more obvious after the adsorption of $Cu^{2+}$. This suggests that effective degradation bacteria might be more resistant to the combined pollution of TPT and metal ions.

**Supplementary Materials:** The following are available online at http://www.mdpi.com/2227-9717/7/6/358/s1, Figure S1. Morphology of *B. thuringiensis* during the quick contact process. (a) Control; (b) PBS; (c) TPT solution; (d) 50 $mg{\cdot}L^{-1}$ Tween 80 solution. Figure S2. Histogram of Young's modulus and adhesion force frequency distribution of *B. thuringiensis* during the quick contact process. Figure S3. Histogram of Young's modulus and adhesion force frequency of *B. thuringiensis* during the conventional contact process. Figure S4. Surface morphology of *B. thuringiensis* after $Cu^{2+}$ biosorption during TPT biodegradation. Table S1. Effect of time on degradation and removal of TPT. Table S2. Correlation between adhesion force of *B. thuringiensis* and PT degradation. Table S3. Correlation between adhesion force, molecular weight, and molecular size. Table S4. Functional proteins related to copper in *B. thuringiensis.*

**Author Contributions:** Conceptualization, Y.L.; Supervision, H.Q. and X.L.; Writing—original draft, H.Z.; Writing—review & editing, J.Y.

**Funding:** This research was funded by the National Natural Science Foundation of China, grant number 21577049, the Science and Technology Project of Guangdong Province, grant number 2016B02024007 and the Fundamental Research Funds for the Central Universities, grant number, 21617453.

**Conflicts of Interest:** The authors declare that they have no conflict of interest.

## References


1. Liu, L.L.; Wang, J.T.; Chung, K.N.; Leu, M.Y.; Meng, P.J. Distribution and accumulation of organotin species in sea water, sediment sand organisms collected from a Taiwan mariculture area. *Mar. Pollut. Bull.* **2011**, *63*, 535–540. [CrossRef] [PubMed]
2. De Carvalho Oliveira, R.; Santelli, R.E. Occurrence and chemical speciation analysis of organotin compounds in the environment: A review. *Talanta* **2010**, *82*, 9–24.
3. Zhao, Y.J.; He, J.C.; Chen, Q.; He, J.; Hou, H.Q.; Zheng, Z. Evaluation of 206 nm UV radiation for degrading organometallics in waste water. *Chem. Eng. J.* **2011**, *167*, 22–27. [CrossRef]
4. Podratz, P.L.; Merlo, E.; Sena, G.C.; Morozesk, M.; Bonomo, M.M.; Matsumoto, S.T.; da Costa, M.B.; Zamprogno, G.C.; Brandao, P.A.; Carneiro, M.T.; et al. Accumulation of organotins in sea food leads to reproductive tract abnormalities in female rats. *Reprod. Toxicol.* **2015**, *57*, 29–42.
5. Cole, R.F.; Mills, G.A.; Parker, R.; Bolam, T.; Birchenough, A.; Kröger, S.; Fones, G.R. Trends in the analysis and monitoring of organotins in the aquatic environment. *Trends Environ. Anal. Chem.* **2015**, *8*, 1–11. [CrossRef]
6. Gao, J.; Ye, J.; Ma, J.; Tang, L.; Huang, J. Biosorption and biodegradation of triphenyltin by *Stenotrophomonas* maltophilia and their influence on cellular metabolism. *J. Hazard. Mater.* **2014**, *276*, 112–119. [CrossRef] [PubMed]
7. Ye, J.; Yin, H.; Peng, H.; Bai, J.; Xie, D.; Wang, L. Biosorption and biodegradation of triphenyltin by *Brevibacillus brevis*. *Bioresour. Technol.* **2013**, *129*, 236–241.
8. Huang, J.; Ye, J.; Ma, J.; Gao, J.; Chen, S.; Wu, X. Triphenyltin biosorption, dephenylation pathway and cellular responses during triphenyltin biodegradation by *Bacillus thuringiensis* and tea saponin. *Chem. Eng. J.* **2014**, *249*, 167–173. [CrossRef]
9. Tang, L.; Wang, L.; Ou, H.; Li, Q.; Ye, J.; Yin, H. Correlation among phenyltins molecular properties, degradation and cellular influences on *Bacillus thuringiensis* in the presence of biosurfactant. *Biochem. Eng. J.* **2016**, *105*, 71–79.
10. Wang, L.; Yi, W.; Ye, J.; Qin, H.; Long, Y.; Yang, M.; Li, Q. Interactions among triphenyltin degradation, phospholipid synthesis and membrane characteristics of *Bacillus thuringiensis* in the presence of d-malic acid. *Chemosphere* **2017**, *169*, 403–412. [CrossRef]
11. Li, Y.; Li, C.; Qin, H.; Yang, M.; Ye, J.; Long, Y.; Ou, H. Proteome and phospholipid alteration reveal metabolic network of *Bacillus thuringiensis* under triclosan stress. *Sci. Total Environ.* **2018**, *615*, 508–516.
12. Zhou, P; Chen, Y.; Lu, Q.; Qin, H.; Ou, H.; He, B.; Ye, J. Cellular metabolism network of *Bacillus thuringiensis* related to erythromycin stress and degradation. *Ecotoxicol. Environ. Saf.* **2018**, *160*, 328–341. [CrossRef] [PubMed]
13. Yi, X.; Bao, V.W.W.; Leung, K.M.Y. Binary mixture toxicities of triphenyltin with tributyltin or copper to five marine organisms:Implications on environmental risk assessment. *Mar. Pollut. Bull.* **2017**, *124*, 839–846. [CrossRef] [PubMed]
14. Wang, N.; Zhang, M.; Chang, Y.; Niu, N.; Guan, Y.; Ye, M.; Li, C.; Tang, J. Directly observing alterations of morphology and mechanical properties of living cancer cells with atomic force microscopy. *Talanta* **2019**, *191*, 461–468. [CrossRef] [PubMed]
15. Plodinec, M.; Loparic, M.; Monnier, C.A.; Obermann, E.C.; Zanetti-Dallenbach, R.; Oertle, P.; Hyotyla, J.T.; Aebi, U.; Bentires-Alj, M.; Schoenenberger, C.-A.; et al. The Nanomechanical Signature of Breast Cancer. *Biophys. J.* **2013**, *104*, 321a.
16. Dufrene, Y.F.; Ando, T.; Garcia, R.; Alsteens, D.; Martinez-Martin, D.; Engel, A.; Gerber, C.; Muller, D.J. Imaging modes of atomic force microscopy for application in molecular and cell biology. *Nat. Nanotechnol.* **2017**, *12*, 295–307.
17. Van Der Hofstadt, M; Huttener, M.; Juarez, A.; Gomila, G. Nano scale imaging of the growth and division of bacterial cells on planar substrates with the atomic force microscope. *Ultramicroscopy* **2015**, *154*, 29–36.
18. Tarafdar, A; Sarkar, T.K.; Chakraborty, S.; Sinha, A.; Masto, R.E. Biofilm development of *Bacillus thuringiensis* on MWCNT buckypaper: Adsorption-synergic biodegradation of phenanthrene. *Ecotoxicol. Environ. Saf.* **2018**, *157*, 327–334. [CrossRef]

19. Harimawan, A; Rajasekar, A.; Ting, Y.P. Bacteria attachment to surfaces–AFM force spectroscopy and physicochemical analyses. *J. Colloid Interface Sci.* **2011**, *364*, 213–218. [CrossRef]
20. Zhang, T; Chao, Y.; Shih, K.; Li, X.Y.; Fang, H.H. Quantification of the lateral detachment force for bacterial cells using atomic force microscope and centrifugation. *Ultramicroscopy* **2011**, *111*, 131–139. [CrossRef]
21. Adams, E.L.; Almagro-Moreno, S.; Boyd, E.F. An atomic force microscopy method for the detection of binding forces between bacteria and a lipid bilayer containing higher order gangliosides. *J. Microbiol. Methods* **2011**, *84*, 352–354. [CrossRef] [PubMed]
22. Doktycz, M.J.; Sullivan, C.J.; Hoyt, P.R.; Pelletier, D.A.; Wu, S.; Allison, D.P. AFM imaging of bacteria in liquid media immobilized on gelatin coated mica surfaces. *Ultramicroscopy* **2003**, *97*, 209–216. [CrossRef]
23. Ye, J.; Zhao, H.; Yin, H.; Peng, H.; Tang, L.; Gao, J.; Ma, Y. Triphenyltin biodegradation and intracellular material release by *Brevibacillus brevis*. *Chemosphere* **2014**, *105*, 62–67. [CrossRef] [PubMed]
24. Ye, J.; Yin, H.; Mai, B.; Peng, H.; Qin, H.; He, B.; Zhang, N. Biosorption of chromium from aqueous solution and electroplating waste water using mixture of Candida lipolytica and dewatered sewage sludge. *Bioresour. Technol.* **2010**, *101*, 3893–3902. [CrossRef] [PubMed]
25. Ortiz, A; Teruel, J.A.; Aranda, F.J. Effect of triorganotin compounds on membrane permeability. *Biochim. Biophys. Acta* **2005**, *1720*, 137–142. [CrossRef] [PubMed]
26. Wang, L.; Ye, J.; Ou, H.; Qin, H.; Long, Y.; Ke, J. Triphenyltin recognition by primary structures of effector proteins and theprotein network of *Bacillus thuringiensis* during the triphenyltin degradation process. *Sci. Rep.* **2017**, *7*, 4133.
27. Oves, M; Khan, M.S.; Zaidi, A. Biosorption of heavy metals by *Bacillus thuringiensis* strain OSM29 originating from industrial effluent contaminated north Indian soil. *Saudi J. Biol. Sci.* **2013**, *20*, 121–129. [CrossRef]
28. Pardo, R; Herguedas, M.; Barrado, E.; Vega, M. Biosorption of cadmium, copper, lead and zinc by inactive biomass of Pseudomonas Putida. *Anal. Bioanal. Chem.* **2003**, *376*, 26–32. [CrossRef]
29. Zhang, Y.; Miller, R.M. Effect of a Pseudomonas rhamnolipid biosurfactant on cell hydrophobicity and biodegradation of octadecane. *Appl. Environ. Microbiol.* **1994**, *60*, 2101–2106.
30. Yi, W; Li, C.; Ye, J.; Long, Y.; Qin, H. Correlation between triphenyltin degradation and cellular metabolic responses of *Bacillus thuringiensis*. *Int. Biodeterior. Biodegrad.* **2017**, *122*, 61–68. [CrossRef]
31. Özer, A.; Gürbüz, G.; Çalimli, A.; Körbahti, B.K. Biosorption of copper(II) ions on Enteromorpha prolifera: Application of response surface methodology (RSM). *Chem. Eng. J.* **2009**, *146*, 377–387.